Modelling uncontrolled solar drying of mango waste

Wilkins, R, Brusey, J & Gaura, E

Original citation & hyperlink:
Wilkins, R, Brusey, J & Gaura, E 2018, 'Modelling uncontrolled solar drying of mango waste' *Journal of Food Engineering*, vol 237, pp. 44-51.
https://dx.doi.org/10.1016/j.jfoodeng.2018.05.012

DOI 10.1016/j.jfoodeng.2018.05.012
ISSN 0260-8774

Publisher: Elsevier

Modelling uncontrolled solar drying of mango waste

Ross Wilkins[a], James Brusey[a,*], Elena Gaura[a]

[a] *Faculty of Engineering and Computing, Coventry University, Coventry, CV1 5FB, United Kingdom*

Abstract

Kiln-dried fruit drying time is readily predicted from initial moisture content since the environment is tightly controlled. For uncontrolled environments, such as a greenhouse solar dryer, a product's drying time varies depending on ambient conditions and is thus more difficult to predict. Prediction of the drying time is needed to better schedule dryer use. Data was obtained from a set of wireless scales that weigh the waste during solar drying after initial moisture content measurement of a sample. A set of linear and quadratic models for drying rate are tested with the best yielding a 39% reduction in RMSE over traditional models. The results indicate that the modelling approach is likely to be useful for open solar dryers where the temperature, and thus the drying rate, is not controlled.

Keywords: Internet of Things, solar drying, drying kinetics, drying rate, fruit drying

1. Introduction

Solar drying is an inexpensive method of drying materials containing moisture, such as fruit. However, solar drying is an uncontrolled process; changes in temperature, wind, humidity and solar load have the potential to significantly alter drying time and thus disrupt the production schedule. Many researchers (see Kucuk et al. [1] for a recent review) model solar drying by deriving a drying rate coefficient from empirical data, however,

1. commonly used drying models do not account for environmental conditions, such as temperature,
2. where temperature is considered, model coefficients are generally derived in well-controlled laboratory-based experiments, which may not be representative of factory conditions,

*Corresponding author

Email addresses: ross.wilkins@coventry.ac.uk (Ross Wilkins), j.brusey@coventry.ac.uk (James Brusey), e.gaura@coventry.ac.uk (Elena Gaura)

3. cross-validation is rarely used to evaluate the reported models, since only one or two batches are dried.

In principle, incorporating environmental parameters into the drying model will improve its accuracy. There are two benefits to a more accurate estimate of the drying rate: it enables accurate prediction of drying *time* (when the product will reach a target moisture content), thus helping scheduling; and it potentially leads to less variation in the final moisture content, thus improving the quality of the final product.

This paper presents a drying model that takes into account varying air temperature by modelling drying rate rather than moisture content. The coefficients of the drying rate model are derived from data collected from a live factory environment, which was instrumented to allow long-term monitoring of mango waste drying (Section 3). The contributions of this work are:

1. To empirically derive the relationship between moisture equilibrium and temperature and show the subsequent impact of temperature on drying rate (Section 4);
2. To derive drying rate model coefficients from uncontrolled, in-situ experiments, where several parameters are changing throughout the experiment (Section 5);
3. To show that the resulting drying model significantly outperforms several commonly used models (Section 5).

2. Related Work

The theoretical modelling of the drying process stems from the observation (attributed to Fick [2]) that evaporation of water is a diffusion process and thus, is based on random molecular motions. This leads to the notion that evaporative drying is analogous to transfer of heat. Specifically (according to Crank [3]),

$$F_x = -D\frac{\partial C}{\partial x} \tag{1}$$

where F_x is the rate of transfer of mass per unit section (or flux) in the direction of the x axis ($\mathrm{kg\,m^{-2}\,s^{-1}}$), C is the concentration ($\mathrm{kg\,m^{-3}}$), and D is the diffusivity ($\mathrm{m^2\,s^{-1}}$). Intuitively, Eq. 1 says that a substance flows away from areas of high concentration and towards areas of low concentration.

When considering surface evaporation for an object (e.g., a sphere) with an initially uniform concentration, evaporation rate is proportional to the difference between surface concentration C_s and the concentration C_e required to maintain equilibrium with the outside air,

$$-D\frac{\partial C}{\partial r} = \alpha\left(C_s - C_e\right) \tag{2}$$

where r is the distance (in m) from the centre of the sphere [3, 4].

Concentration C refers to mass per unit volume. When considering evaporation, it is common to assume that the sample does not shrink as it dries [4]. Thus, its volume is based only on the mass and density ρ of dry matter and so concentration C is proportional to the dry basis moisture content M, or $\rho M = C$, giving,

$$-D\frac{\partial M}{\partial r} \quad = \quad \alpha\left(M_s - M_e\right) \tag{3}$$

Similar equations can be formed for different material shapes but, most commonly, it is assumed that the material being dried is a thin sheet and that drying occurs from both sides. Crank [3, (4.18)] gives the solution for diffusion in a plane sheet as,

$$MR = \frac{8}{\pi^2}\sum_{n=0}^{\infty}\frac{1}{z\left(n\right)}\exp\left\{-z(n)\cdot kt\right\} \tag{4}$$

where $z\left(n\right) = \left(2n+1\right)^2$, $k = \pi^2 D/\left(4l^2\right)$, and l is half the sheet thickness. Note that the solution in Eq. 4 makes some simplifying assumptions about the material.

Moisture ratio MR is defined as the ratio between the current and initial moisture differences with the equilibrium, or,

$$MR = \frac{M_t - M_e}{M_0 - M_e} \tag{5}$$

Many researchers [5, 6, 7, 8, 9, 10, 11, 12, 13] have approximated Eq. 4 by dropping all but the first term to yield an equation of the form,

$$MR \approx \frac{8}{\pi^2}\exp\left(-kt\right) \tag{6}$$

which has the added attraction that it is time invariant (i.e., t can be mapped to $t+a$ if M_0 is adjusted accordingly). Note that it is usually helpful, given that t is remapped, to drop the $8/\pi^2$ term and normalise so that $MR = 1$ at $t = 0$. This is a reasonably accurate approximation of Eq. 4 but only after the initial fast phase of drying. The initial phase occurs when the moisture content is roughly uniform across the cross-section and there is a large drop in moisture content at the boundary. This might occur, for example, just after the fruit has been cut open. For many cases, including for the application examined here, the initial phase has already completed before monitoring begins.

The above formulation ignores environmental effects, such as air temperature, solar radiation, humidity, and air flow rate. In this work, the focus is on the effect of air temperature on drying rate.

2.1. Environmental effects

The most common approach to incorporating temperature into the drying model is via diffusivity. For example, Babalis and Belessiotis [6] and Srivastava

[13] assume that diffusivity varies with temperature according to the Arrhenius equation typically used for chemical reaction rates,

$$D = D_0 \exp\left(\frac{-E_a}{RT}\right) \tag{7}$$

where E_a is the activation energy (J); R is the universal gas constant ($\mathrm{J\,K^{-1}}$); and T is the temperature in kelvin. However, here the activation energy affects how large a change in diffusivity is caused by a unit change in temperature. From an empirical modelling point of view, this may be unnecessarily restrictive and some works avoid this restriction by finding an empirical linear mapping between temperature and k in Eq. 6.

In addition to affecting diffusivity, air temperature (and relative humidity) can alter the point M_e at which moisture content of the sample reaches equilibrium with its environment. Considering M_e to be related to temperature (and humidity) is a useful approach since it allows us to model the fact that at low temperatures (and high humidities), the drying process can reverse, with moisture being reabsorbed from the surrounding air. Note that temperature and relative humidity are usually highly correlated.

Surprisingly, equilibrium moisture content M_e is often disregarded (and considered zero) [14, 7, 9, 15, 16, 17, 13, 18]. The reasoning often given is that, for solar drying, the environment varies and thus so does M_e. Furthermore, an argument is made that M_e is close to zero. In some works, the Guggenheim, Anderson, de Boer (GAB) equation is used to demonstrate that M_e is near zero [6]. Dissa et al. [19] derive their own formula for M_e based on relative humidity and temperature, however, some details of this formula are missing (e.g., T_4 is referenced but it is not clear what temperature this refers to). According to El-Sebaii et al. [20], Henderson provides the following relationship between temperature, relative humidity RH and M_e,

$$1 - RH = \exp\left(-cTM_e^n\right) \tag{8}$$

where c and n are empirical constants for a particular product. In addition, they use an empirical linear relationship between the drying constant k and temperature. Despite these small exceptions, the dominant approach in the literature is to assume M_e is zero.

As will be shown, *M_e is actually a significant factor in estimating drying rate.* Furthermore, *it is possible to find the relationship between M_e and temperature even when these are varying throughout the experiment.*

2.2. Empirical models

In comparison to the theoretical models provided by Crank [3], many works posit a variety of simpler, empirically derived models. As Simal et al. [21] points out, such models do not necessarily provide insight into the underlying physics of the drying process; they are, however, useful because they predict drying behaviour accurately.

Kucuk et al. [1] provide an extensive review of such works and note a total of 67 different models. Although there are variations, the most popular models correspond to Eq. 6.

The general approach to identifying the drying model parameters is to:

1. Measure the initial moisture content of a sample.
2. Weigh the drying sample at regular intervals throughout the drying process.
3. Identify the equilibrium moisture content M_e (based on the weight when drying stops). Note that this step is typically skipped (M_e assumed to be zero) but even when included, M_e is assumed to be constant throughout the drying process.
4. Derive the estimated moisture content.
5. Fit to one or more models.
6. Test. Typical statistical tests include correlation coefficient, R^2, Root Mean Square Error (RMSE), and χ^2 but Kucuk et al. [1] note a total of 28 different measures used on the resulting fit. The tests are used to select the best model to fit the available data.

Notably, apart from Erenturk and Erenturk [22], cross-validation is absent from the statistical tests in step 6 and this is typically due to only one or two drying batches being used to fit the model. Cross-validation might be helpful in two ways: first, it helps identify problems with overfitting caused by too complex a model with too many parameters; second, it provides a more realistic estimate of the predictive performance of the model.

Kucuk et al. [1] also note that measurement uncertainty analysis is important but rarely performed. This analysis is useful (Section 5.1) since it identifies that the resulting models are sensitive to variation in initial moisture content.

2.3. Solar dryer design

A key factor in the solar drying performance is the design of the dryer. The simplest type is the open solar dryer, where the product is dried on a bed open to sun and wind.

Tunnel or greenhouse dryers provide shelter from rain and keep off insects. Janjai et al. [23] rigorously examine the cost-effectiveness of a solar greenhouse with solar photovoltaic fans. They measured solar radiation, temperature, relative humidity (every 10 minutes) and product weight (4 times per day) during the drying process. They show that, compared with open air solar drying, the solar greenhouse produces a higher quality product with a shorter drying time. Sacilik et al. [24] also compared a solar tunnel dryer with open sun drying and were able to show several benefits for the former.

In comparison to Janjai et al. [23], Hahn et al. [25] look at much smaller scale solar greenhouses and recirculate air after drying it with silica gel desiccant. They compared fan drying of Roselle with hybrid solar-biogas methods and found the latter to be faster and produce better results.

Fadhel et al. [26] compare open air versus solar dryer and solar tunnel greenhouse for chilli. They note that the solar dryer is the best performer but say that the greenhouse could be made competitive if indoor air humidity can be reduced.

Indirect-type solar dryers heat air in a solar collector section. This air is then ducted to a kiln where products are placed to be dried. Usually, natural convection provides sufficient airflow but sometimes a chimney is added. A variation on this design, examined by Smitabhindu et al. [27], is to put the solar collector on the rooftop and the kiln underneath. A Liquefied petroleum gas burner provides supplementary heat to bring the air temperature to 60 °C. This approach smooths the kiln temperature over time.

To avoid variability due to diurnal cycles, Solar Dryers Australia developed a large scale solar kiln for drying wood, seeds, and nuts that stores heat during the day and releases through the night. Smoothing the diurnal variation has clear advantages over simply modelling it, however their approach requires additional infrastructure and thus may not be suitable in all situations.

The point here is that there are a variety of different types of solar dryers with different levels of technological sophistication. Greenhouse solar dryers, such as the one examined in this work, are more subject to changes in environmental conditions but require little infrastructure. An alternative approach, not examined in this work, is to augment the dryer with additional heating or somehow reduce the effect of varying environmental conditions. Such additional infrastructure is not always feasible and so being able to model uncontrolled solar dryers is still useful.

2.4. Summary

In summary,

- Drying science is only loosely based on theory and most work in this domain is around empirically selected and parameterised models.
- Although some works identify the effect of temperature on drying rate, such drying experiments tend to be performed in a tightly controlled laboratory environment. Where temperature effects are considered, they are usually incorporated as an effect on diffusivity D.
- Variation in equilibrium moisture content M_e is usually ignored and such terms discarded.
- The greenhouse dryer is at the low-end of technological sophistication but is commonplace and thus it is important to model its behaviour.

3. Materials and Methods

The solar dryer, shown in Figure 1, used in this work is an open air brick building ($30 \times 25 \times 3\,\mathrm{m}^3$) with a transparent polycarbonate roof. Within the solar dryer, there are a total of 36 drying racks (each $5.6 \times 1.2 \times 2\,\mathrm{m}^3$) with 5 drying shelves spaced vertically at 0.4 m intervals. The mango waste is dried on

Figure 1: The solar dryer is based on a large rectangular area covered with a polycarbonate transparent roof.

these shelves as a thin layer. The base of each shelf is made from nylon mesh netting to let sunlight penetrate lower levels and improve airflow.

The solar-dryer is uncontrolled, and only heated by solar. Within the solar dryer temperatures range between 26 °C and 52 °C and relative humidity varies between 42% and 61%. Between the top of a drying shelf (2 m high) and the lower shelf (0.6 m high) there can be a difference of 20 °C and 20% relative humidity.

A custom scale was developed to measure the weight of the mango waste during drying (Figure 2). The scale is based on a Raspberry Pi combined with: a single load cell (TAL201), temperature sensor (DS18B20), an LCD screen, and a WiFi dongle. The load cell has a measurement resolution of 1 g with a measurement range of 0–10 kg. The Raspberry Pi is interfaced with an LCD screen, which displays current weight measurements. Data is buffered and then transmitted hourly to a remote server. A Kern MLS-A Moisture Analyser was used to measure moisture content of small samples.

Data analysis was performed using the R statistical language, using lm for multiple linear regression, the modelr package for cross-validation and the caret package for artificial neural networks (ANNs).

3.1. Data collection procedure

Five scales were deployed between April and July 2016. The scales were deployed in different locations within the solar dryer at various rack heights.

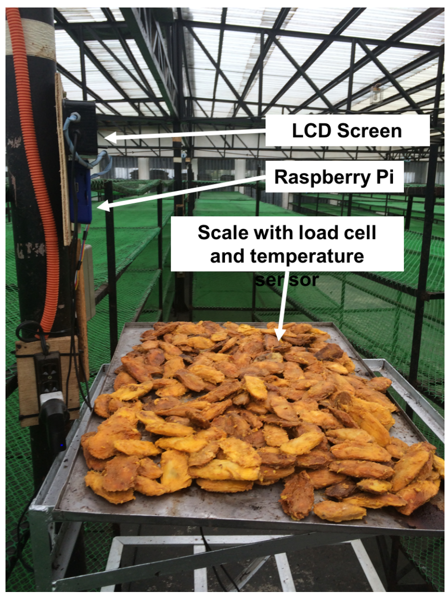

Figure 2: Each instrumented shelf consists of a metal tray (shown here loaded with mango kernels) with a central load cell and temperature sensor. The load cell is attached to a signal conditioning unit and Raspberry Pi that displays current measurements on an LCD and transmits product weight and air temperature data periodically via WiFi to a central server.

During this deployment period, the scales monitored a total of 18 batches of mango seed over a total of 67 drying days.

The process of drying a batch of mango was conducted as follows:

1. An average of 3.5 kg (SD: 0.7 g, max: 5.72 kg, min: 2.99 kg) of mango seeds were placed on a scale's drying tray in a single layer.
2. A sample seed was taken from the tray at loading time and the moisture content was measured using the moisture analyser. Over all batches, the mango seed average initial (wet basis) moisture content was 64% (SD: 6%, max: 72%, min: 51%).
3. Weight and local air temperature measurements were taken automatically by the custom scale at 2 s intervals throughout the drying process for each batch.
4. The mango seeds were left to dry on the scales until the factory operators deemed the mango to be dry. The drying time for the mango was between 3–10 days.

The data collected and used for the modelling here is available at `http://cogentee.coventry.ac.uk/datasets/pulp2017`.

4. Development of a drying rate model

The problem faced when modelling drying in a solar dryer is illustrated in Figure 3, which shows that the change of weight over time is not a simple function of time. Two key effects are evident. First, each day there is a diurnal variation such that drying slows during the night and accelerates during the day. Second, as water is lost, the drying rate, for the same hour of the next day, is reduced. Figure 4 shows that the diurnal variation is common to all batches studied.

The diurnal variation could be due to a change in diffusivity D, a change in moisture equilibrium M_e, or both. This work, in contrast to past work, considers the effect of variation in M_e. From Eq. 5,

$$M_t = (M_0 - M_e)\exp(-kt) + M_e \tag{9}$$

which has differential form,

$$\frac{dM_t}{dt} = (M_e - M_t)\,k \tag{10}$$

M_e varies with environmental conditions such as temperature, humidity, and airflow. Since airflow was consistently low in the greenhouse, and since humidity tends to vary with temperature, it is assumed that M_e is a function of temperature only.

Although temperature varies throughout the day, it is possible to select data points where the temperature is close to a particular value, as shown in Figure 5 for temperatures around 30 °C. Equilibrium moisture content M_e for that temperature can then be determined from the intersection of the line fit

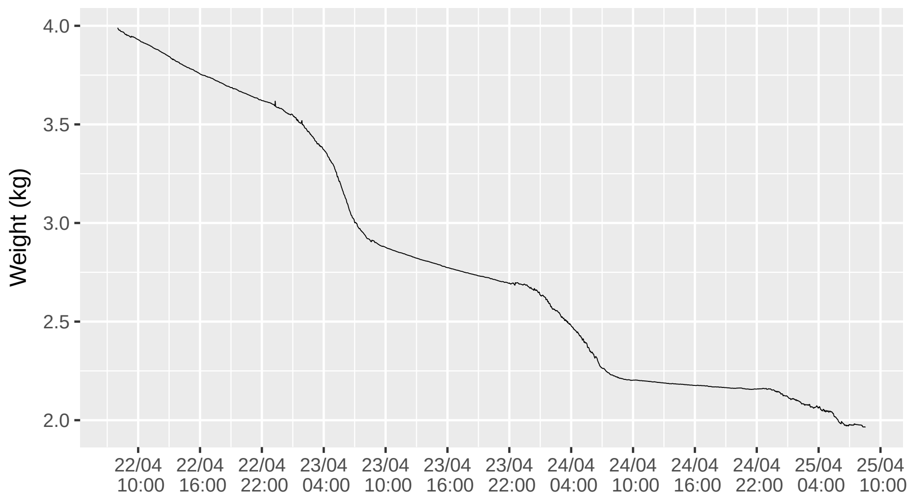

Figure 3: Mango seed weight decreases during drying at a variable rate (slow at night and fast during the day).

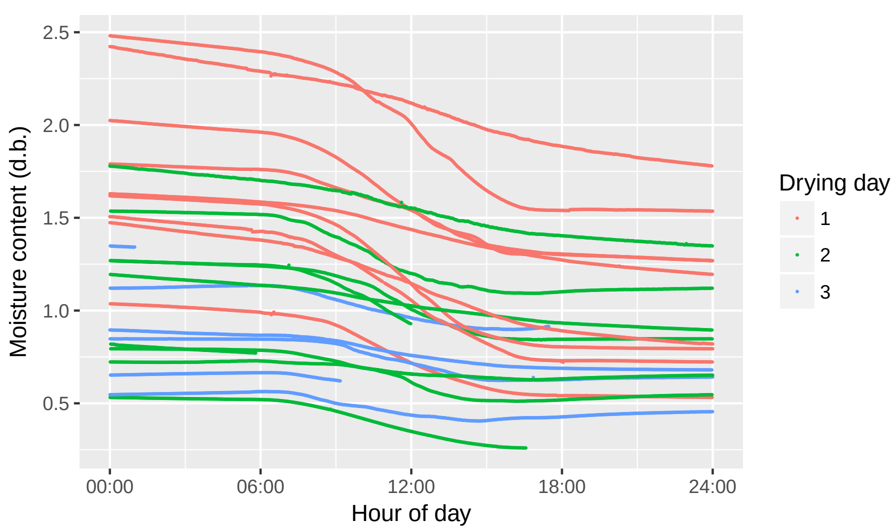

Figure 4: Moisture content (d.b.) reduces most during the middle of the day but the gradient does not just depend on those two variables, as indicated by crossing over of lines for different batches.

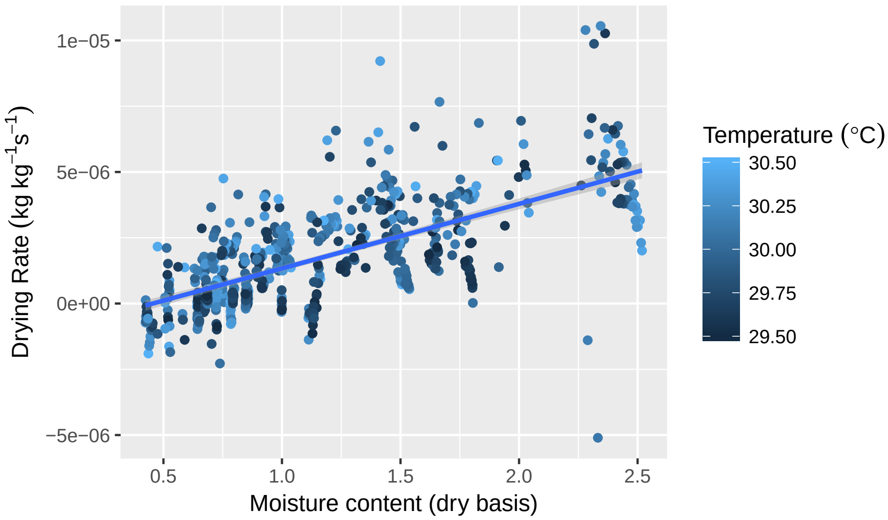

Figure 5: For a particular temperature, drying rate $-\frac{dM_t}{dt}$ varies linearly with moisture content M_t. The equilibrium moisture M_e is at the intersection of the line fit with the x-axis.

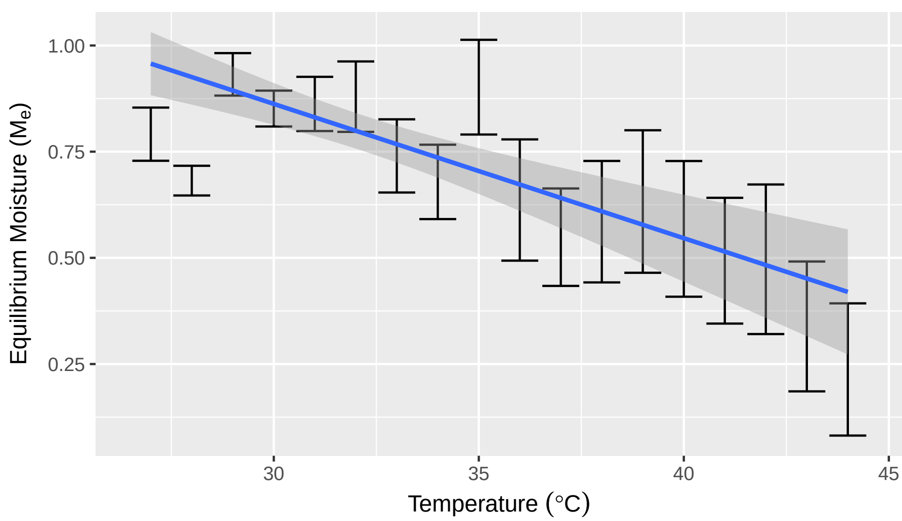

Figure 6: By using a series of fits as per Figure 5 for different temperatures and plotting the fit intercept (or equilibrium moisture content M_e), a roughly linear relationship with temperature emerges. Error bars show 95% confidence interval for each intercept.Temperatures with few data points have been excluded.

with the x-axis. By performing the line fit between moisture content and drying rate for different temperatures, a linear correspondence between equilibrium moisture M_e and temperature emerge, as shown in Figure 6. Thus, a linear correspondence between equilibrium moisture and temperature,

$$M_e = \alpha T + \beta \tag{11}$$

combined with Eq. 10 leads to,

$$\frac{dM}{dt} = (\alpha T + \beta - M_t)\, k \tag{12}$$

Since temperature T varies with time stochastically, there is no analytical solution in terms of M_t. Fortunately, it is possible to estimate the drying rate $-\frac{dM}{dt}$ and solve for the corresponding multi-linear model. As noted previously, diffusivity D, and thus k, is also a function of temperature T. Assuming a linear relationship leads to,

$$\frac{dM}{dt} = (\alpha T + \beta - M_t)\,(aT + b) \tag{13}$$

Furthermore, it is possible to take into account the drying tray position. Note that if the drying tray position is significant, it indicates that some factor, such as airflow or solar radiance, that has not be accounted for, is influencing performance.

A set of linear and non-linear models were generated based on:

- models from the literature that are suitable to be expressed in terms of drying rate as a function of moisture content (Newton and Henderson) rather than moisture content as a function of time.
- the above analysis that justifies terms based on the effect of M_e and D assuming they are linear with respect to air temperature (MoTe and MoTe2X).
- variants with additional higher power (e.g., to allow for a non-linear relationship between M_e and T) including Mote2 and / or *influence* terms denoted with an "X", including MoTeX, MoTe2X, etc. Influence terms are those involving multiplication of two different input variables.
- variants that include the scale location (using one-hot encoding) including MoTeSc, MoTeScX, etc.

Furthermore, two ANN variants were trained (with and without scale location). The resulting set of possible models is summarised in Table 1.

5. Fitting the data to model set

Prior to fitting the models in Table 1, scale measurement data was preprocessed as follows:

Table 1: The following set of models are tested. For compactness, R formula conventions are used, such that $A \sim B + C \times D$ corresponds to the linear equation $A = c_0 + c_1 B + c_2 C + c_3 D + c_4 CD$. Where the intercept c_0 is fixed to zero, this is written $0 + \ldots$

Name	Model
Newton [28]	$\frac{dM}{dt} \sim 0 + M$
Henderson [29]	$\frac{dM}{dt} \sim M$
MoTe	$\frac{dM}{dt} \sim M + T$ or Eq. 12
MoTe2	$\frac{dM}{dt} \sim M + T + T^2$
MoTe2X	$\frac{dM}{dt} \sim M \times \left(T + T^2\right)$ or Eq. 13
MoTeX	$\frac{dM}{dt} \sim M \times T$
MoTeSc	$\frac{dM}{dt} \sim M \times T + S$
MoTeScX	$\frac{dM}{dt} \sim M \times T \times S$
Mo2Te2X	$\frac{dM}{dt} \sim M \times T \times M^2 \times T^2$
Mo2Te2ScX	$\frac{dM}{dt} \sim M \times T \times M^2 \times T^2 \times S$
ANN [22]	$\frac{dM}{dt} = f(M, T)$
ANN (with scale)	$\frac{dM}{dt} = f(M, T, S)$

1. Invalid (outside sensor range) weight measurements were removed.
2. Data was split into batches based on recorded mango waste loading/unloading times.
3. For some batches, a weight offset was applied to short periods to correct for temporary addition or removal of weight.
4. Dry basis moisture content at each time point M_t was calculated from the initial (wet basis) moisture content W_0 and the initial and current mass m_0, m_t, according to,

$$M_t = \frac{m_t - (1 - W_0)\, m_0}{(1 - W_0)\, m_0} \tag{14}$$

5. Drying rate is estimated as $-\Delta M_t / \Delta t$ and all terms are smoothed by taking the mean over a 30 min window.

Following this, models are fitted (using R's LM fit or CARET's neural network trainer).

Results shown in Figure 7 and Table 2 are based on 10-fold cross validation (the models were trained on a random selection of 90% of the data, tested on the remaining 10%; repeated 10 ways).

The RMSE performance for each model is shown as a box-plot in Figure 7 and this is also shown numerically in Table 2 along with the adjusted R^2 statistic for the fit. Traditional models (Newton and Henderson) perform relatively poorly for our mango waste drying scenario. Adding a term for temperature (as per Eq. 12) improves performance but further gains are possible by including influence terms ($M \times T$) as suggested by Eq. 13. Since including terms for the scale location improves performance, this suggests that some other factor in the environment, such as airflow, differs between different scale locations. Furthermore, measuring this additional factor might then improve the model.

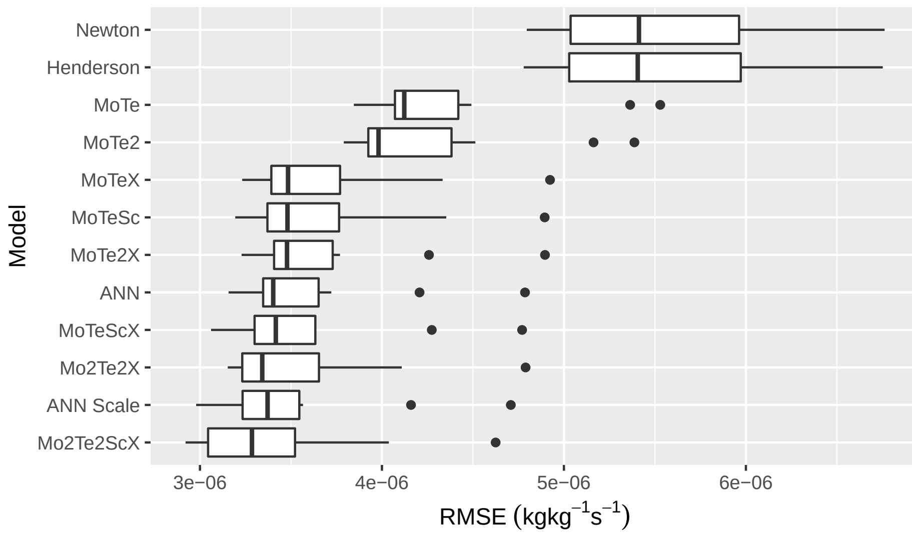

Figure 7: The RMSE performance from 10-fold cross validation for each model. Traditional models (Newton and Henderson) perform relatively poorly compared to models including a temperature term.

Adding quadratic terms further improves performance with model Mo2Te2ScX providing peak performance. Notably, ANN performs slightly worse than the best linear model, however, it is possible that meta parameter tuning could help (e.g., adjusting hidden weights).

In summary, the performance of the best models reflect the assertion that equilibrium moisture content M_e and diffusivity D are affected by temperature and including terms for both effects in the model significantly improves accuracy. Furthermore, since including the scale location in the model improves performance, some other location dependent or experimental factor (other than moisture content or temperature) must affect the drying rate. Therefore, humidity, solar irradiance, and airflow might need to be measured to further improve model accuracy.

5.1. Measurement uncertainty

Table 3 gives the uncertainties for measured parameters. Measurement uncertainty analysis provides two types of information. First, it highlights those measurements that contribute significantly to uncertainty in the final estimate. Second, it provides an overall budget for the uncertainty in a derived value.

Where there is a measurement system $y = f(x_1, x_2, \ldots)$ with various component uncertainties $U_{x_1}, U_{x_2}, \ldots$, the total or aggregate uncertainty is

$$U_y^2 = \sum_i \left(\frac{\partial f(\bar{x}_i)}{\partial x_i} U_{x_i} \right)^2 \quad (15)$$

Table 2: RMSE and adjusted coefficient of determination (R^2) values for 10-fold cross validation testing

Model	Adjusted R^2	RMSE ($kg\,kg^{-1}\,s^{-1}$)
Henderson	0.093 ± 0.003	$5.6 \times 10^{-6} \pm 8 \times 10^{-7}$
Newton	0.415 ± 0.004	$5.6 \times 10^{-6} \pm 8 \times 10^{-7}$
MoTe	0.44 ± 0.011	$4.3 \times 10^{-6} \pm 8 \times 10^{-7}$
MoTe2	0.47 ± 0.011	$4.2 \times 10^{-6} \pm 8 \times 10^{-7}$
MoTe2X	0.60 ± 0.014	$3.6 \times 10^{-6} \pm 9 \times 10^{-7}$
MoTeSc	0.60 ± 0.014	$3.6 \times 10^{-6} \pm 8 \times 10^{-7}$
MoTeX	0.60 ± 0.014	$3.7 \times 10^{-6} \pm 8 \times 10^{-7}$
MoTeScX	0.62 ± 0.014	$3.5 \times 10^{-6} \pm 9 \times 10^{-7}$
Mo2Te2X	0.63 ± 0.014	$3.5 \times 10^{-6} \pm 8 \times 10^{-7}$
Mo2Te2ScX	0.67 ± 0.014	$3.4 \times 10^{-6} \pm 8 \times 10^{-7}$

Table 3: Measurement uncertainties based on 95th percentile confidence intervals (or U_{95}) are given below for measurement instruments. Uncertainty information comes from either the instrument *data sheet* (type B), is *calculated* (type B; based on number of bits being stored), is *estimated* (type B; for weights where traceable calibration was unavailable), or found *experimentally* (type A; based on variance in a large number of batches). Type A sources are assumed to be normally distributed while type B sources are assumed to be rectangular.

Measurement	Source	Uncertainty (U_{95})
Temperature		0.29 K
Sensor accuracy	Data sheet	0.29 K
ADC conversion (24 bit)	Calculated	0.000 006 K
Temperature variation	Experiment	0.035 K
Weight		2.9 g
Calibration weights	Estimated	0.012 g
Load cell sensor noise	Experiment	0.008 g
ADC conversion (14 bit)	Calculated	0.35 g
Effect of temperature	Experiment	2.9 g
Moisture content		5.8%
Moisture analyser	Data sheet	0.012%
Moisture analyser output rounding	Data sheet	0.0029%
Variation in mango seed	Experiment	5.8%

where $\bar{x}_i$ is a nominal value where the gradient $\frac{\partial f}{\partial x_i}$ is found. For example, the aggregate uncertainty budget for temperature measurement is,

$$
\begin{aligned}
U_T &= \left(0.29^2 + 0.000006^2 + 0.035^2\right)^{1/2} \\
&\approx 0.29\,\mathrm{K}
\end{aligned}
$$

Note that, in this case, the gradients $\frac{\partial f}{\partial x_i}$ for components are all 1. Similarly, aggregate uncertainty for moisture content and weight measurement are shown in Table 3.

Given the definition of dry basis moisture M_t in Eq. 14, and assuming nominal values $m_t = 2\,\mathrm{kg}$, $W_0 = 65\%$, $m_0 = 4\,\mathrm{kg}$, the moisture content uncertainty is $U_{M_t} = 0.116\,\mathrm{kg\,kg^{-1}}$.

Note that the uncertainty in initial wet basis moisture content is the largest contributor. This is mainly due to the variation in initial moisture content for samples in a single batch.

Taking MoTe2X (Eq. 13), for example, the uncertainty in the final drying rate estimate $\frac{dM_t}{dt}$ is similarly found to be $9.1 \times 10^{-7}\,\mathrm{kg\,kg^{-1}\,s^{-1}}$ on the basis of partial derivatives for moisture content and temperature, and assuming nominal values $M = 1.1$, $T = 33$.

This result suggests that the measurement uncertainty is much smaller than the cross-validation RMSE for MoTe2X ($3.5 \times 10^{-6}\,\mathrm{kg\,kg^{-1}\,s^{-1}}$) and thus measurement contributes only slightly to the overall uncertainty in the model. A difficulty with this view is that the model is a non-linear function of inputs and thus the choice of nominal values is critical to the measurement uncertainty budget estimate. Our view is that the cross validation result is likely to be more representative. A key finding from the uncertainty analysis is that the dry basis moisture estimate, and thus the drying rate prediction is most sensitive to the initial moisture content measurement.

6. Conclusions and future work

This work departs from past approaches in a number of ways.

1. Rather than produce a temporal model of moisture content for solar drying of mango waste, this work models in terms of drying rate explicitly. This has the advantage that time varying parameters, such as temperature, can be accounted for. The resulting drying model outperforms those existing in the literature.
2. It examines the impact of air temperature on the moisture equilibrium of mango seed and show that there is a roughly linear relationship between the two for the temperature ranges considered.
3. This work demonstrates, in contrast to much of the work in the literature, that even when the equilibrium moisture varies, it should not be ignored. The relationship between moisture content and environmental parameters that affect it can be derived if a sufficiently large number of drying runs are available.

4. Model coefficients are derived from uncontrolled, in-situ experiments, where several parameters are changing throughout the experiment, rather than controlled, laboratory ones.

In future work, we will examine the impact of changes to the configuration of the greenhouse (such as increasing ventilation or altering height of shelving). We also plan to incorporate automatic data collection and display of estimated drying times into the factory operation in order to (a) collect a much larger corpus of data and (b) ensure product is dried more accurately and efficiently.

Acknowledgements

Part of the research leading to these results has received funding from the British Councils's Newton Fund Institutional Links Grant Agreement under grant agreement n° 172732595. We acknowledge the support of Prof. Evelyn Taboada and Edward Querikiol of the University of San Carlos, The Philippines and operations staff from Green Enviro Management Systems Inc for help with data collection.

References

[1] H. Kucuk, A. Midilli, A. Kilic, I. Dincer, A Review on Thin-Layer Drying-Curve Equations, Drying Technology 32 (7) (2014) 757–773, ISSN 0737-3937, doi:10.1080/07373937.2013.873047.

[2] A. Fick, On liquid diffusion (reprinted), Journal of Membrane Science 100 (1) (1995) 33 – 38, ISSN 0376-7388, doi:https://doi.org/10.1016/0376-7388(94)00230-V, URL `http://www.sciencedirect.com/science/article/pii/037673889400230V`, the early history of membrane science selected papers celebrating vol. 100.

[3] J. Crank, The mathematics of diffusion, Oxford Univ. Press (1975) 414ISSN 03064549, doi:10.1016/0306-4549(77)90072-X.

[4] S. Janjai, B. Mahayothee, N. Lamlert, B. K. Bala, M. Precoppe, M. Nagle, J. Müller, Diffusivity, shrinkage and simulated drying of litchi fruit (Litchi Chinensis Sonn.), Journal of Food Engineering 96 (2) (2010) 214–221, ISSN 02608774, doi:10.1016/j.jfoodeng.2009.07.015.

[5] E. K. Akpinar, Mathematical modelling of thin layer drying process under open sun of some aromatic plants, Journal of Food Engineering 77 (4) (2006) 864–870, ISSN 02608774, doi:10.1016/j.jfoodeng.2005.08.014.

[6] S. J. Babalis, V. G. Belessiotis, Influence of the drying conditions on the drying constants and moisture diffusivity during the thin-layer drying of figs, Journal of Food Engineering 65 (3) (2004) 449–458, ISSN 02608774, doi:10.1016/j.jfoodeng.2004.02.005.

[7] E. Correa-Hernando, F. J. Arranz, B. Diezma, E. Juliá, J. I. Robla, L. Ruiz-Garcia, J. García-Hierro, P. Barreiro, Development of model based sensors for the supervision of a solar dryer, Computers and Electronics in Agriculture 78 (2) (2011) 167–175, ISSN 01681699, doi:10.1016/j.compag.2011.07.004.

[8] A. O. Dissa, H. Desmorieux, P. W. Savadogo, B. G. Segda, J. Koulidiati, U. Claude, B. Lyon, Shrinkage, porosity and density behaviour during convective drying of spirulina, Journal of Food Engineering 97 (3) (2010) 410–418, ISSN 0260-8774, doi:10.1016/j.jfoodeng.2009.10.036.

[9] A. El-Beltagy, G. R. Gamea, A. H. A. Essa, Solar drying characteristics of strawberry, Journal of Food Engineering 78 (2) (2007) 456–464, ISSN 02608774, doi:10.1016/j.jfoodeng.2005.10.015.

[10] R. P. F. Guiné, D. M. S. Ferreira, M. J. Barroca, F. M. Gonçalves, Study of the drying kinetics of solar-dried pears, Biosystems Engineering 98 (4) (2007) 422–429, ISSN 15375110, doi:10.1016/j.biosystemseng.2007.09.010.

[11] A. A. Kabiru, A. A. Joshua, A. O. Raji, Effect of Slice Thickness and Temperature on the Drying Kinetics of Mango (Mangifera Indica), International Journal of Recent Research and Applied Studies 15 (1) (2013) 41–50.

[12] K. B. Koua, W. F. Fassinou, P. Gbaha, S. Toure, Mathematical modelling of the thin layer solar drying of banana, mango and cassava, Energy 34 (10) (2009) 1594–1602, ISSN 03605442, doi:10.1016/j.energy.2009.07.005.

[13] A. K. Srivastava, Modeling and Evaluation of Thermal Diffusivity and Activation Energy of Potato slices in Forced Convection Multi Tray Solar Dryer, American Journal of Food Science and Technology 3 (2) (2015) 27–32, doi:10.12691/ajfst-3-2-1.

[14] E. K. Akpinar, Drying of mint leaves in a solar dryer and under open sun: Modelling, performance analyses, Energy Conversion Management 51 (12) (2010) 2407–2418, ISSN 01968904, doi:10.1016/j.enconman.2010.05.005.

[15] Z. Erbay, F. Icier, A Review of Thin Layer Drying of Foods: Theory, Modeling, and Experimental Results, Critical Reviews in Food Science and Nutrition 50 (5) (2010) 441–464, ISSN 1040-8398, doi:10.1080/10408390802437063.

[16] S. H. Khodabakhsh Aghdam, A. R. Yousefi, M. Mohebbi, S. M. A. Razavi, A. Orooji, M. R. Akbarzadeh-Totonchi, Modeling for drying kinetics of papaya fruit using fuzzy logic table look-up scheme, International Food Research 22 (3) (2015) 1234–1239, ISSN 22317546.

[17] B. Paul, S. P. Singh, Design , development and performance evaluation of solar dryer with mirror booster for red chilli (capsicum annum), International Journal of Engineering Trends and Technology 5 (1) (2013) 25–31, ISSN 2231-5381.

[18] P. P. Tripathy, S. Kumar, A methodology for determination of temperature dependent mass transfer coefficients from drying kinetics: Application to solar drying, Journal of Food Engineering 90 (2) (2009) 212–218, ISSN 02608774, doi:10.1016/j.jfoodeng.2008.06.025.

[19] A. O. Dissa, D. J. Bathiebo, H. Desmorieux, O. Coulibaly, J. Koulidiati, U. Claude, B. Lyon, Experimental characterisation and modelling of thin layer direct solar drying of Amelie and Brooks mangoes, Energy 36 (5) (2011) 2517–2527, ISSN 03605442, doi:10.1016/j.energy.2011.01.044.

[20] A. A. El-Sebaii, S. Aboul-Enein, M. R. I. Ramadan, H. G. El-Gohary, Empirical correlations for drying kinetics of some fruits and vegetables, Energy 27 (9) (2002) 845–859, ISSN 03605442, doi:10.1016/S0360-5442(02) 00021-X.

[21] S. Simal, A. Femenia, M. C. Garau, C. Rosselló, Use of exponential, Page's and diffusional models to simulate the drying kinetics of kiwi fruit, Journal of Food Engineering 66 (3) (2005) 323–328, ISSN 02608774, doi:10.1016/j.jfoodeng.2004.03.025.

[22] S. Erenturk, K. Erenturk, Comparison of genetic algorithm and neural network approaches for the drying process of carrot, Journal of Food Engineering 78 (3) (2007) 905–912, ISSN 02608774, doi:10.1016/j.jfoodeng.2005.11.031.

[23] S. Janjai, P. Intawee, J. Kaewkiew, C. Sritus, V. Khamvongsa, A large-scale solar greenhouse dryer using polycarbonate cover: Modeling and testing in a tropical environment of Lao People's Democratic Republic, Renewable Energy 36 (3) (2011) 1053–1062, ISSN 09601481, doi:10.1016/j.renene.2010.09.008.

[24] K. Sacilik, R. Keskin, A. K. Elicin, Mathematical modelling of solar tunnel drying of thin layer organic tomato, Journal of Food Engineering 73 (3) (2006) 231–238, ISSN 02608774, doi:10.1016/j.jfoodeng.2005.01.025.

[25] F. Hahn, G. Hernández, J. Hernández, C. Pérez, J. M. Vargas, Optimization of roselle drying time and drying quality, Canadian Biosystems Engineering 53 (3) (2011) 1–8, ISSN 14929058.

[26] A. Fadhel, S. Kooli, A. Farhat, A. Belghith, Experimental Study of the Drying of Hot Red Pepper in the Open Air, under Greenhouse and in a Solar Drier, International Journal of Renewable Energy and Biofuels 2014 (2014) (2014) 1–14, ISSN 23330589, doi:10.5171/2014.515285.

[27] R. Smitabhindu, S. Janjai, V. Chankong, Optimization of a solar-assisted drying system for drying bananas, Renewable Energy 33 (7) (2008) 1523–1531, ISSN 09601481, doi:10.1016/j.renene.2007.09.021.

[28] W. K. Lewis, The Rate of Drying of Solid Materials, J. Ind. Eng. Chem. 13 (5) (1921) 427–432, ISSN 0095-9014, doi:10.1021/ie50137a021.

[29] S. Henderson, S. Pabis, Grain drying theory I. Temperature effect on drying coefficient, J. Agric. Eng. Res. 6 (3) (1961) 169–174.